Sampling Tool Concepts for Enceladus Lander In-situ Analysis

Mircea Badescu
Jet Propulsion Laboratory,
California Institute of Technology
4800 Oak Grove Dr.
Pasadena, CA 91109
818-393-5700
Mircea.Badescu@jpl.nasa.gov

Paul Backes
Jet Propulsion Laboratory,
California Institute of Technology
4800 Oak Grove Dr.
Pasadena, CA 91109

Scott Moreland
Jet Propulsion Laboratory,
California Institute of Technology
4800 Oak Grove Dr.
Pasadena, CA 91109

Alexander Brinkman
Jet Propulsion Laboratory,
California Institute of Technology
4800 Oak Grove Dr.
Pasadena, CA 91109

Dario Riccobono
Politecnico di Torino, Department of Mechanical and Aerospace Engineering, Corso Duca degli Abruzzi 24, 10129 Torino (Italy)

Matthew Dotson
Jet Propulsion Laboratory,
California Institute of Technology
4800 Oak Grove Dr.
Pasadena, CA 91109

Noel Csomay-Shanklin
Jet Propulsion Laboratory,
California Institute of Technology
4800 Oak Grove Dr.
Pasadena, CA 91109

Samuel Ubellacker
Jet Propulsion Laboratory,
California Institute of Technology
4800 Oak Grove Dr.
Pasadena, CA 91109

Jamie Molaro
Jet Propulsion Laboratory,
California Institute of Technology
4800 Oak Grove Dr.
Pasadena, CA 91109

Mathieu Choukroun
Jet Propulsion Laboratory,
California Institute of Technology
4800 Oak Grove Dr.
Pasadena, CA 91109

Giancarlo Genta
Politecnico di Torino, Department of Mechanical and Aerospace Engineering, Corso Duca degli Abruzzi 24, 10129 Torino (Italy)

Abstract— **A potential future in-situ lander mission to the surface of Enceladus could be the lowest cost mission to determine if life exists beyond Earth since material from the subsurface ocean, where the presence of hydrothermal activity has been strongly suggested by the Cassini mission, is available on its surface after being ejected by plumes and then settling on the surface. In addition, the low radiation environment of Enceladus would not significantly alter the chemical makeup of samples recently deposited on the surface. A study was conducted to explore various sampling devices that could be used by an in-situ lander mission to provide 1cc to 5cc volume samples to instruments. In addition to temperature and vacuum environmental conditions, the low surface gravity of Enceladus (1% of Earth gravity) represents a new challenge for surface sampling that is not met by sampling systems developed for microgravity (e.g., comets and asteroids) or higher gravity (e.g., Europa 13%g, Moon 16%g, or Mars 38%g) environments. It is desired to acquire surface plume material that has accumulated in the top 1cm to ensure acquisition of the least processed material. Several sampling devices were developed or adapted and then tested in simulated conditions that resemble the Enceladus surface properties. These devices and test results are presented in this paper.**

TABLE OF CONTENTS

1. INTRODUCTION 1
2. SIMULANTS 2
3. LANDER STABILITY ANALYSIS 3
4. TESTBED 4
5. FULL FACE BIT 4
6. DRIVE TUBE 5
7. ULTRASONIC SCOOP 7
8. RASP SAMPLING SYSTEM 8
9. SAMPLE TRANSFER 10
10. CONCLUSIONS AND FUTURE WORK 11
ACKNOWLEDGEMENTS 11
REFERENCES 11
BIOGRAPHY 12

978-1-5386-6854-2/19/$31.00 ©2019 IEEE

1. INTRODUCTION

A potential future in-situ mission to the surface of Enceladus could be the lowest cost landed mission to determine if life exists beyond Earth since material from the subsurface ocean, where the presence of hydrothermal activity has been strongly suggested by the Cassini mission, is available on its surface after being ejected by plumes and then settling on the surface. In addition, the low radiation environment of Enceladus would not significantly alter the chemical makeup

of samples recently deposited on the surface. Sampling on Enceladus presents temperature and vacuum environmental challenges. The low surface gravity of Enceladus (1% of Earth gravity) represents a new challenge for surface sampling that is not met by sampling systems developed for microgravity (e.g., comets and asteroids) or higher gravity (e.g., Europa 13%g, Moon 16%g, or Mars 38%g) environments. A study was conducted to explore various sampling devices that could be used by an in-situ lander mission to provide to instruments 1cc to 5cc volume samples of plume material that has accumulated in the top 1cm to ensure acquisition of the least processed material. We focused mainly on devices that operate with a low reaction force, entail low energy consumption, are robust to low gravity and are compatible with stringent contamination control requirements. Several sampling devices were developed or adapted and then tested in simulated conditions that resemble the Enceladus surface properties.

The potentially strong material of 12MPa unconfined compressive strength (UCS) precludes the use of sampling tools that only work for weak materials such as the TAGSAM sampler of the OSIRIS-REx mission or the CAESAR comet surface sample return mission sampling system [Squyres, 2018]. The low 8N reacted force to the lander objective precludes use of sampling tools that require higher reacted loads such as the Mars Science Laboratory powder drill (300N preload) and the proposed Europa Lander mission baseline counter-rotating saws and rasp (with currently assumed 50N maximum reacted loads). The BiBlade [Backes, 2014] developed for comet surface sampling and Brush Wheel Sampler [Bonitz, 2012] developed for asteroid surface sampling were designed for higher reacted loads that are available in a touch-and-go mission architecture where spacecraft inertia reacts sampling forces. The Rosetta mission Philae lander rotary drill, SD2 [Finzi, 2007], would only acquire very weak material, and as a drill, would be poorly suited for collecting surface material [Backes, 2014]. The Phobos Grunt mission had the CHOMIK percussive drive tube sampler [Seweryn, 2010], but as a drive tube it is designed to primarily collect subsurface samples.

2. SIMULANTS

The study was started with the objective of producing physical simulants representative of the surface of Enceladus by investigating related micron-scale ice particle sintering [Molaro, 2018]. The Enceladus surface environment provides unique sampling system constraints. Findings from the Cassini mission and sintering research indicate an Enceladus surface of anticipated 40-95% porosity and strength range of 400 kPa to 12 MPa UCS [Molaro, 2018]. Simulants were developed to support testing the sampler prototypes described in this paper. The design and production of the mechanical strength simulant was based on the description of potential Enceladus surface microstructure morphology. These simulants were intended to be preliminary and to aid in early sampler testing prior to intensive study of laboratory ice analogues. We chose the simulant parameters based on our best understanding of Enceladus' range of possible surface properties, and we specifically considered the needs of the sampling tools we're developing (e.g., considering strong and very weak materials for worst case scenarios) in making these choices.

The simulants were developed to have the following microstructure properties: Granular, cohesive type bulk structure; micro structure to be of particles bonded to neighboring touching particles (i.e., necking type shape to contacting particles); ~10-100um grain size with narrow size range (poorly graded); rounded or sub-rounded particle shape; particles of high strength material; particle-particle bonding method to be high strength and brittle while maintaining adequate minimum necking and porosity; brittle failure; 35 to 45% porosity.

A specific value of strength was not prescribed since laboratory measurements of Enceladus icy analogues have not been made. There are efforts currently underway at JPL to produce such analogs and to measure strength in-situ within the environmental chamber where ice is produced and evolved.

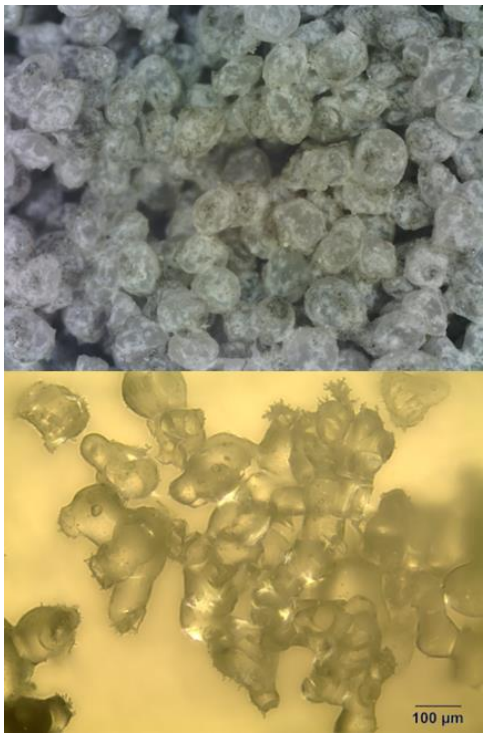

Figure 1. "Pervious" concrete simulant (Top), Sintered cryogenic ice (Bottom).

Four "pervious" concrete mixes were selected as simulants. Two were "very fine-grain" of ~100um mean particle size and two were "fine-grain" of ~400um mean particle size. Each of the grain size simulants had a 2.5MPa and 4.5MPa UCS (unconfined compressive strength, 2in cube in compression) strength version of the mix.

3. LANDER STABILITY ANALYSIS

The next objective of this study was to analyze the stability of the lander and determine the allowable reaction load from a sampling device. Microgravity missions, such as OSIRIS REx to an asteroid and the proposed CAESAR mission to a comet, rely on relatively high maximum reacted sampling loads due to the touch-and-go mission architecture that uses the momentum of the spacecraft to react sampling loads (up to 1000s of N). The higher gravity environments for landed missions to the moon, Mars, Venus, and Europa allow for higher maximum reacted load requirements, e.g., 300N for the Mars Science Laboratory rover powder drill. The baseline 410kg Europa lander provides an assumed maximum allowable 50N reacted force to the lander. An Enceladus lander of Europa lander mass and the same 11:1 ratio of local weight to preload would allow for only 4.3N of reacted force for sampling. We proposed and performed preliminary tests on sublimating posts on the lander legs which would enable a higher objective of 8N maximum reacted load to the lander. Sample contamination objectives are expected to be similar to those of a Europa Lander mission since both planetary bodies have the potential to harbor life. The low energy use objective is similar to a Europa Lander objective since these missions would likely be constrained to use battery power on the landers.

The very low surface gravity of Enceladus represents a new challenge for surface sampling. Even small forces applied to the lander (e.g. forces generated by a sampling system and transmitted through a robotic arm) could weaken its equilibrium state, potentially causing the lander to lift or slide downhill. Therefore, a critical task is the evaluation of the effect of the forces the sampling system might apply to the lander while performing the sampling operations. A three-dimensional analytical model was developed to study the static equilibrium of the lander with the aim to determine the static equilibrium envelope within which the sampling tool should be designed. In particular, the model provides an indication on the maximum allowed magnitude of the sampling force that prevents the lander changing its equilibrium state. The model computes the three Cartesian components of the reaction forces acting on each of the four legs of the lander (Fig. 2). This approach allows the evaluation of the lander's reaction to generic external loads having components along all three Cartesian axes. The model assumes the lander behaves as a rigid body, while the point of contact between each lander leg and the ground is modeled via three springs along the three Cartesian axes. The model gives the chance to change several parameters related to the environment (e.g., gravity acceleration, slope of the ground), the lander (e.g., mass, shape/dimensions/height of the body, legs length, leg-to-ground friction coefficient) and the sampling operation (e.g., sampling spot, magnitude of the sampling force/torque, inclination of the sampling force/torque with respect to the ground). The analysis of different types of sampling systems (e.g., scoops, drills, buckets, etc.) was done by varying the parameters related with the sampling operations. The model computes the three reaction forces for each leg by solving a non-linear system of twelve equations, composed by six equilibrium conditions and six geometric conditions. The static equilibrium envelope is defined as the envelope within which the reaction forces acting on the lander legs are within a defined margin. Two types of margins are considered. The first type of margin is computed upon the smallest leg-to-ground friction force and is applied to the X and Y components of the reaction forces.

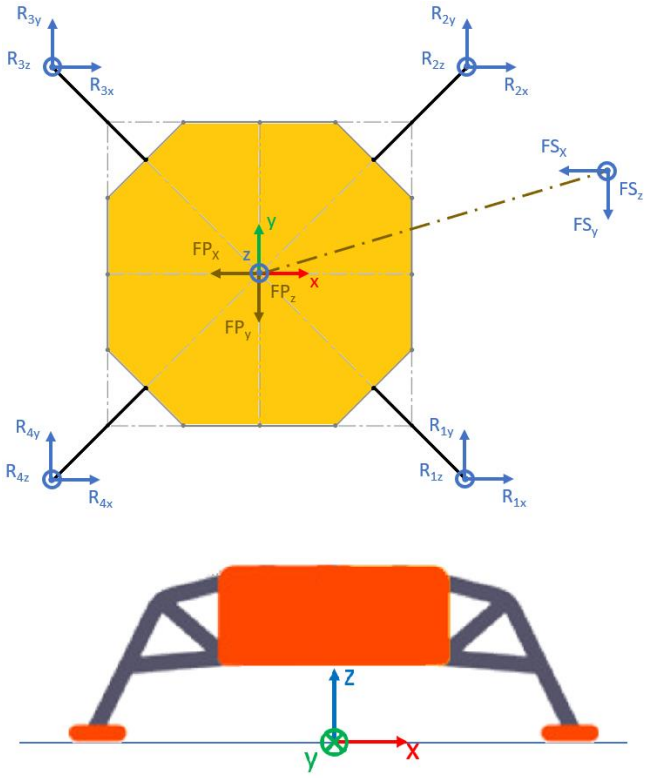

Figure 2. Top view of the lander (top) with the indication of the reaction forces on the legs, the weight force FP and the sampling force FS. Front view of the lander (bottom) with the indication of the reference system.

The second type of margin is computed upon the null value of the Z component of the reaction force, which represents the condition for the incipient lifting of the leg. An iterative process is required to compute the static equilibrium envelope. Since this iterative process implies solving a non-linear system of equations at each iteration, the computational cost/time can be significantly high, especially considering the most general case. For this reason, a minimization algorithm was applied to find the max allowed magnitude of the sampling force. Moreover, a sensitivity analysis was conducted to find the parameters having the most influence on the max allowed magnitude of the sampling force. The less sensitive parameters were found to be the dimensions and the height of the lander body. Moreover, the values of the less sensitive parameters, the sampling tool inclination with respect to the ground and the margin were considered constant across the analysis. The most sensitive parameters were found to be the lander mass, the sampling spot and the leg-to-ground friction coefficient. Those parameters were

varied across the analysis to find different static equilibrium envelopes. Fig. 3 shows the static equilibrium envelope for a scoop-like sampling system.

The addition of small heated pins (6mm diameter x 80mm long) was expected to be utilized for the purpose of increasing resistance to lander footpad sliding. These heated pins create a v-shaped hole in the ice for the pins to rest in. Preliminary laboratory testing showed the interaction can be modelled as a point sliding up a frictionless slope (due to radiation, the walls are not vertical). A conservative value of the slope measured was used in the lander model and input as an equivalent friction coefficient (~0.75). The simplified (single axis) loads plot shows a maximum net resultant with footpad pins as 8N before the lander becomes unstable. This value was used as a requirement for the sampling system in the form as maximum reaction force allowable.

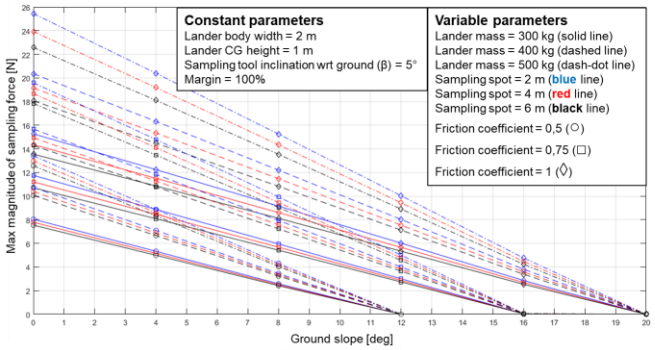

Figure 3. Static equilibrium envelope for a scoop-like sampling system.

4. TESTBED

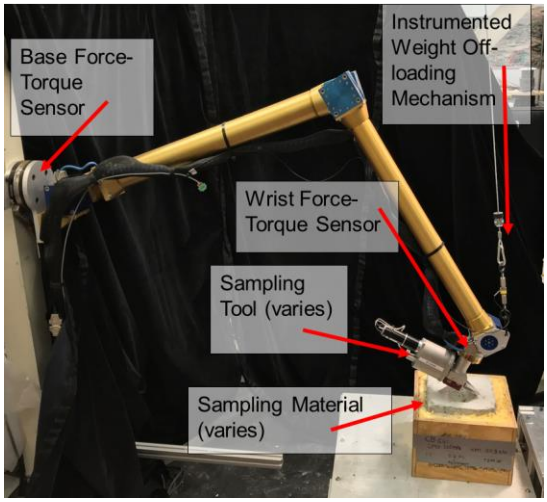

Figure 4. Manipulation testbed showing one of the tested tools

All the sampling tool prototypes were developed to be evaluated in the same testbed. The manipulation testbed consists of a 3 degree-of-freedom robotic arm equipped with two force-torque sensors and a weight offloading mechanism. The force-torque sensors are configured in base-mounted and wrist-mounted locations to understand sampling loads and analyze force signal attenuation through the sampling arm to the lander. The weight off-loading mechanism is used to reduce the joint torques during sampling operations and instrumented with a load cell to enable full free-body load estimation on the arm. The arm has a mounting interface after the wrist force-torque sensor to accommodate a number of various sampling tools (Fig. 4).

The kinematics, controls, and operator interfaces for the manipulation testbed are provided by JPL's Controls and Autonomy for Sample Acquisition and Handling (CASAH) software system [Edelberg, 2018]. Basic arm behaviors, like joint motion and task-space motion, are used to provide a set of motion primitives for sampling operations. Force control behaviors were developed to help limit the arm loads during sampling by slowing down the forward progress of the tool as a function of low-pass filtered wrist forces. Compared to open-loop control, force control showed a 70% load reduction using the front-face concave bit in a low strength simulant and a 13% load reduction using the ultrasonic scoop in the same conditions.

5. FULL FACE BIT

One of the tested tools was a rotary hammer tool with a powder bit with full face cutting ability that drives the cuttings toward the bit rotation axis and stores the cuttings inside the bit. A rotary hammer tool allows operation with low weight-on-bit and low torque. The bit cutting teeth configuration allows for low torque from the driving tool. A conical bit and a cylindrical bit shapes were tested. The cylindrical bit was tested in two teeth arrays configurations and was also designed to enable efficient pneumatic transfer of collected cuttings.

Figure 5. Cylindrical bit with linear teeth array design (top two pictures) and 3D printed metal test bits (bottom two pictures)

In one configuration, the teeth are aligned in straight line segments, parallel to each other and located behind the

symmetry plane going through the central bit axis in the rotation direction (Fig. 5). In between the two rows of teeth there is an additional center tooth to complete the full front face coverage. Locating the teeth behind the symmetry plane causes the cuttings to be driven toward the central axis where the collection holes are located. The offset distance and the rotational speed are design parameters that need to be taken into consideration to assure that the cuttings are driven toward the bit central axis.

The inside of the bit creates a cavity for storing the cuttings during drilling. The top of the bit can be configured with a spring loaded lid and access ports. A spring loaded lid would allow the cuttings to be pushed out of the bit in case of overflowing to prevent compacting cuttings inside the bit. The access ports would allow the bit to interface with other devices for cuttings removal for sample transfer or bit cleaning. The bit has vertical features that allow the impact to be transferred to the cutting teeth more efficiently. During the testing, the bit cavity was filled with cuttings but a lot more cuttings were driven outside the hole (Fig. 6).

Figure 6. Bit with linear teeth arrays testing

In another configuration, the bit frontal face is a concave surface and the teeth placement follow an arc or parabola segment where the angle of the tangent to the locating curve with the central symmetry plane is proportional to the radial distance from the central axis (Fig. 7). Driving the cuttings toward the central axis assures low strength material surface sample collection. The bit was designed with a lid that can shape the internal bit cavity for sample retention during drilling and subsequent pneumatic sample transfer. In a first fabricated configuration for pneumatic sample transfer, the cavity inside the bit is shaped to increase the efficiency of cuttings removal from inside the bit to transfer it to other devices. The bit was able to collect cuttings during the test and the cuttings were transferred using a pneumatic system (Fig. 8). The tool was tested in various simulants ranging from unconsolidated sand to 5.4 MPa UCS with preload measured in the 6 to 10 N. The bit was able to collect sample of 2.2cc to 2.8cc volume.

Figure 7. Curved teeth array bit and lid design (left) and fabricated integrated into a testbed (right)

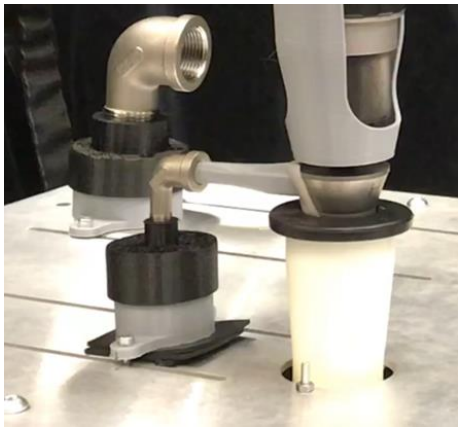

Figure 8. Curved teeth array bit integrated into the sample transfer testbed

6. DRIVE TUBE

Another tested tool was based on a drive tube sampling system for sample collection and transfer. It includes a set of drive tubes, means of driving them into the ground for sample collection, a storage mechanism and means to load them in front of the drive mechanism and a means to transfer them. The main components of the sampling system are shown in Fig. 9 and integrated into a housing in Fig. 10.

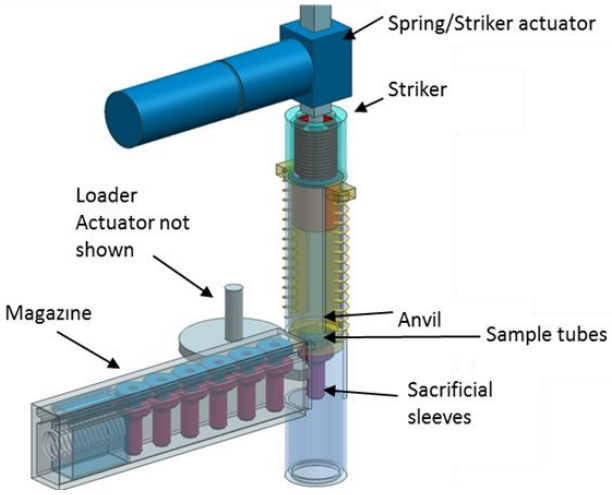

Figure 9. Drive tube sample collection and transfer system main components

The drive tube includes a sample tube, a sample tube sheath and a sample retention mechanism (Fig. 11). The sample tube sheath is shaped as a cylinder with a flange at the top and a through axial hole. At the bottom end, the hole diameter is smaller with a shoulder between the large diameter section and small diameter section. The shoulder can have a groove to aid in the passive control of the sample retaining mechanism shape. The bottom end of the sheath can have chamfers on both inner and outer edges or only on one edge. The chamfers geometry is dictated by the scope of the sheath to collect more or less of the sample material that is being penetrated. The sample tube is shaped as a cylinder with a flange at the upper end to support impact from the anvil and transfer the load to the tip of the sacrificial sheath and tube and to interface with the slot in the anvil. The outer diameter of the sample tube is smaller than the large inner diameter of the sheath and the inner diameter is larger or the same size as the smaller inner diameter of the sheath. At the bottom end, the sample tube has the sample retention mechanism.

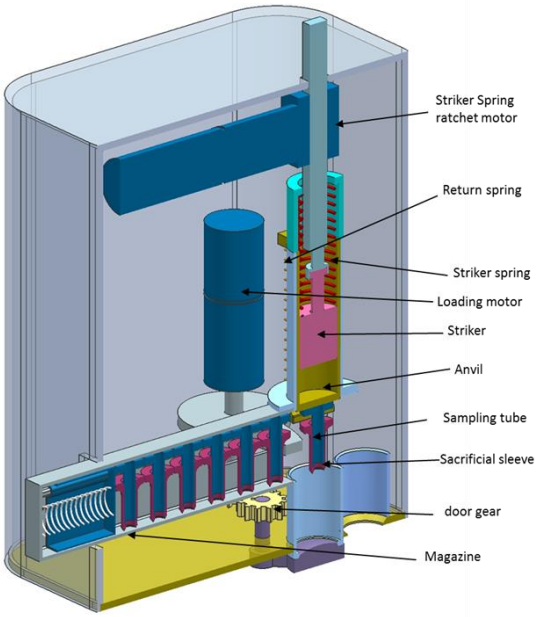

Figure 10. Drive tube sample collection and transfer system main components integrated into a housing

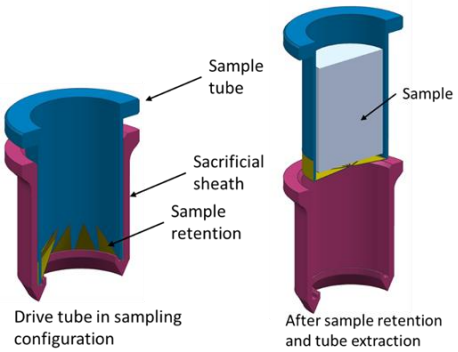

Figure 11. Drive tube in sampling configuration (left) and after sample acquisition and separation (right)

One configuration of the retention mechanism is a fish trap with flexible fingers extending radially from the edge of the sample tube to the central axis. When the sample tube is inserted into the sheath against the bottom sheath shoulder the fingers deform toward the sample tube wall, leaving the central part of the tube open. Having the fingers open allows the tube to sample low penetration resistance material such as fluffy snow or powder. When the sample tube is extracted from the sheath, the fingers are released and retake their relaxed position, closing the bottom opening of the sample tube.

The drive tubes are stored in a linear or circular cartridge where a preloaded spring pushes them toward the drive mechanism axis (Fig. 12). An actuator driven cam mechanism is used to load one drive tube at a time into the drive mechanism, hold the other drive tubes into the cartridge, and slide the sample tube after sampling away from the drive mechanism axis for sample transfer.

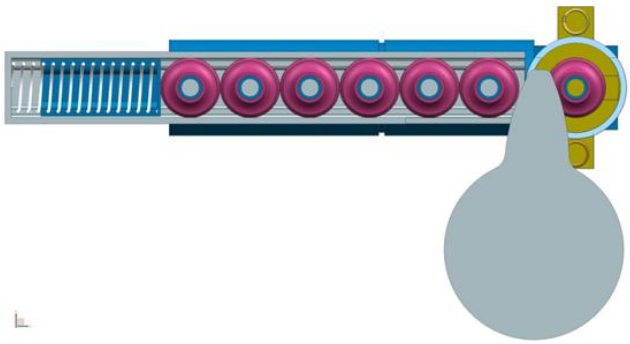

Figure 12. Drive tube storage cartridge

The drive mechanism consists of a guide tube with a bottom baseplate, an anvil with a bottom slot for accommodating the sample tube flange, an extraction spring mounted between the guide tube and the anvil, a hammer and a drive spring, and a linear actuator with a gripper to engage the hammer and preload the drive spring. For sampling, the hammer is retracted to preload the drive spring, a new sample tube is loaded into the anvil slot, and the sampler is placed with the base plate against the surface of the material to be sampled. The hammer is released, the drive spring accelerates the hammer that impacts the anvil and drives the drive tube into the sampled material, preloading the extraction/return spring. The anvil is stopped by the baseplate and the compressed extraction/return spring retrieves the anvil with the sample tube. The sacrificial sheath will remain in the ground during the sample tube extraction. When the sample tube separates from the drive tube sheath, the sample retention mechanism gets activated retaining the sample in the sample tube.

Figure 13. Implemented drive tube components (left) assembled (middle) and sample tube with collected sample (right)

After the sample tube extraction the sampler is docked with the sample receiving station and the sample tube containing the sample is transferred to the sample handling subsystem. The sample can be processed inside the sample tube as is the case for dry volatiles extraction or wet organics extraction. Having the sample enclosed in the sample tube with a known geometry makes the sample handling better determined. Components of the drive tube sampling system were fabricated and tested in the lab (Fig. 13) using an impact mass. The drive tube sampling system can work with an impact driver or a percussive mechanism.

7. ULTRASONIC SCOOP

Another tested tool was a piezoelectric driven sampling device that can collect a predefined volume of sample and requires one degree of freedom for operation. The sampler has two ends where different configuration end-effectors can be attached. In the shown configuration, one end includes a scoop and the other includes a surface preparation tool or chopper (Fig. 14). The piezoelectric actuator is attached to a joint of a robotic arm that can serve as both deployment mechanism and for tool operation. A passive detent driven mechanism can be attached to the same joint as the tool and can serve as a stopper to ease sample collection and function as a scoop lid. The stopper has detent controlled positioning and can be moved in different positions using the joint actuator and the sampling tool.

The tool includes a double-ended piezoelectric actuator that can have different attachments at the two ends, a mounting interface and a stopper mechanism. The piezoelectric actuator includes a single or double piezoelectric stack preloaded between a set of two horns, an interface part for mounting, and different or identical end effector tools attached to the horn tips. The two end effector tools can be run at the horns resonant frequencies and at their own frequency. The piezoelectric stack/s are driven by an AC electric field and can produce oscillations into the horns. The horns geometry can be configured to amplify the stacks vibrations amplitude. The actuator can have an additional mass excited to produce lower frequency higher energy impact to the end effector tools.

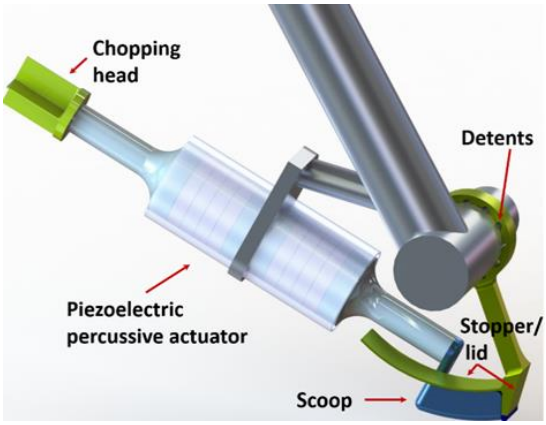

Figure 14. Piezoelectric driven sampling tool

The piezoelectric material used for actuator fabrication can be a material that specifically targets the sampling location environmental conditions such as, for example, cryogenic piezoelectric materials for outer planets sampling and high temperature piezoelectric materials for Venus applications.

In the current implementation, one end effector tool consists of a scoop with curved bottom. The scoop symmetry plane can be mounted inline or offset from the horn symmetry planes. The center of the circle that defines the scoop bottom curvature is configured to be identical with the axis of the mounting joint which allows the device to be operated by only one actuator. The stop link includes the lid rigidly attached to the link. In a different implementation, the lid can be attached to the stop link using a flexure that makes possible the use of a scoop without an axial offset.

The other end-effector tool consists of a chopping tool with flat faces oriented along the piezoelectric actuator axis. This can be used to penetrate the surface and break the material in smaller chunks needed by the science instrument requirements.

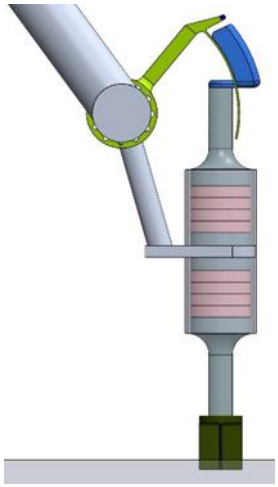

Figure 15. Sampling tool in chopping configuration

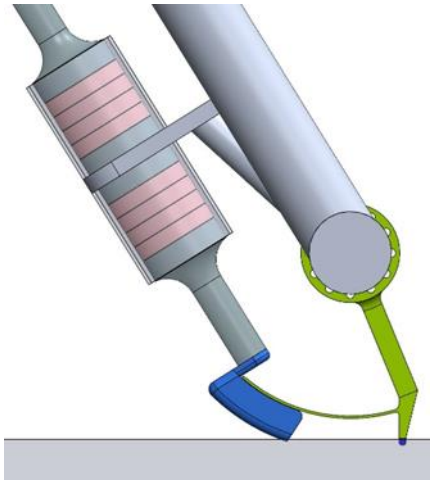

Figure 16. Sampling tool in sampling configuration

For sampling, the following steps can be implemented:
Step 1 – surface preparation (chopping); the deploying robotic arm uses the wrist joint to rotate the tool to move the stop link out of the way and orient the tool with the chopping head against the surface area to be sampled. The piezoelectric tool can be activated to cut slots in the sampling area making it easier for the scoop to collect the sample and pre-sizing the sampled material to the instrument requirements (Fig. 15).

Step 2 – position tool for sampling; the wrist joint rotates the tool to position the stop link in the sampling orientation, then moves the sampling tool away from the stop link. The stop link is loaded against the ground in the sampling area. The tool is rotated so it touches the ground and the lid covers the scoop (Fig. 16).

Step 3 – sampling; the tool has the piezoelectric actuator activated and is rotated using the wrist joint only until it touches the stop link. The wrist joint actuator can be controlled to maintain a maximum applied torque or a predefined rotation speed. The power to drive the piezoelectric actuator can also be controlled (Fig. 17).

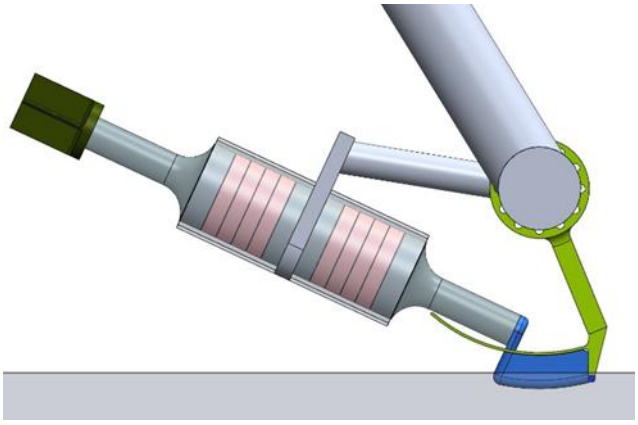

Figure 17. Sampling tool at the end of sample acquisition

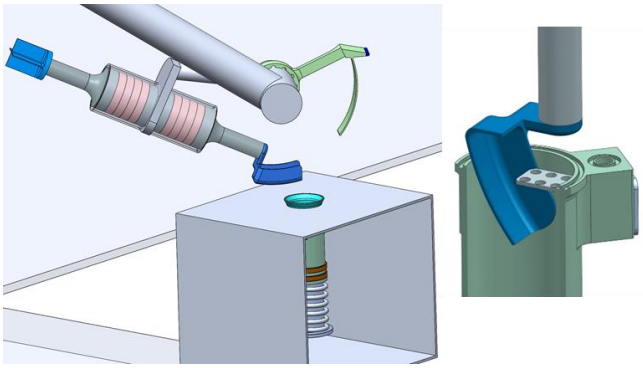

Figure 18. Sampling tool in a sample transfer configuration (left) and scoop being scraped against the sample transfer chamber (right).

Step 4 – sample transfer; after the sampling process is completed, the robotic arm can follow a succession of predefined movements to move the stop link away from a position that would interfere with the sample transfer process while maintaining the scoop in a horizontal position to prevent sample loss. An on-board camera can be used at this time to acquire an image of the scoop with the sample to assess the sample including verifying adequate volume. The scoop is aligned with the delivery location for sample transfer (Fig 18, left). A scraper can be provided at the delivery location so the scoop can be moved against the scraper to remove the collected sample material from the scoop (Fig. 18, right). The piezoelectric actuator can be activated at a lower power level to ease the sample separation from the scoop. After the sample transfer process is completed, the arm can move the tool to a stowing position or perform another sampling operation.

A series of chopping tools configurations were fabricated and tested using two ultrasonic transducers. The tested configurations were flat blade, cross blade, and circular cutter. All cutters were able cut the medium strength consolidated simulant with a preload of 7 to 10N but were not able to penetrate the higher strength simulant (5.4MPa UCS).

8. RASP SAMPLING SYSTEM

A rotary cutter based sampling system was developed and tested. This system relies on high cutter rotational rates to impart momentum into cuttings that are flung into a collection cup located immediately above the spinning cutter. Later the acquired sample can be transferred from the collection cup, and into a container on the lander via a pneumatic system.

The sample collection subsystem of the Rasp for Enceladus application (Fig. 19, 20) is based on the NASA Phoenix Mars Lander Mission Icy Soil Acquisition Device (ISAD) [Bonitz, 2008]. The ISAD consists of a scoop and a rasp bit. The spring loaded rasp bit design and sample cuttings capture strategy was leveraged from this heritage system.

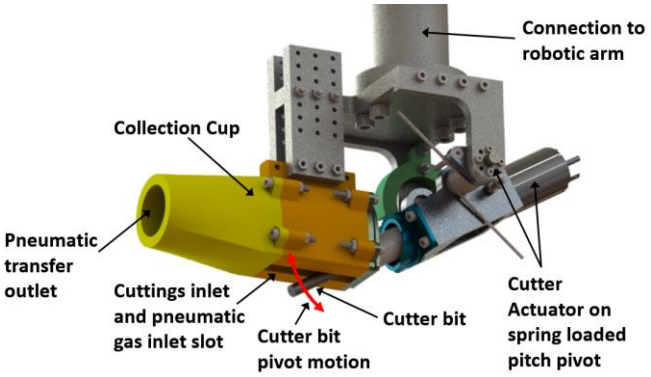

Figure 19. Rasp Sampling System with pneumatic transfer.

A rasp based sampling system is well suited to Enceladus surface sampling application for the following reasons. First, the rasp is robust to excavation and capturing material of a wide range of strength (from loose to very hard). Secondly, the momentum transfer type sample capture, performs increasingly well at lower gravity. The rasp bit easily imparts adequate momentum into excavated particles to fling the material into the collection cup. Lastly, the reaction forces are very low compared to other potential sampling systems while cutting into hard, icy material due to small cutter tooth engagement with the ground and the fly-wheel momentum effect of the high-speed bit.

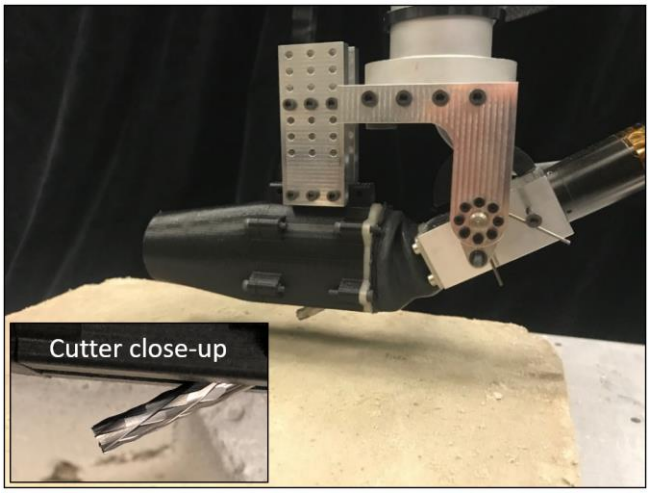

Figure 20. Prototype Rasp Sampling System for Enceladus application. Close-up rotary cutting bit is shown.

Due to the low gravity environment found on Enceladus, dumping of the sample that is located in the collection cup would not be possible. The gravity (~0.01 Earth-g) is sufficiently low that it cannot be relied upon to provide enough force to overcome small scale forces such as electrostatic and friction when attempting to transfer the material out of the sampler and into the potential instrument. The Rasp Sampling System was therefore designed for a pneumatic transfer which is capable of moving the sample in low gravity. The first step in the sample transfer process is to dock the sampler at a location on the lander via the robotic arm (Fig 21-C & Fig 24). This location consists of an instrument cup interface and a gas output interface. The Rasp sampling system docks to both interfaces simultaneously. Only a rough seal is needed at each of the interfaces since the system is designed for pressure system losses and sample losses. The Rasp was demonstrated to meet all requirements including collection of low end and high end strength material. It was tested in unconsolidated material, medium strength and high strength material with a preload of 6 to 8N and was able to collect 1.5cc material. End-to-end sample acquisition and transfer to a mock instrument inlet/cup was successfully demonstrated (Fig 21).

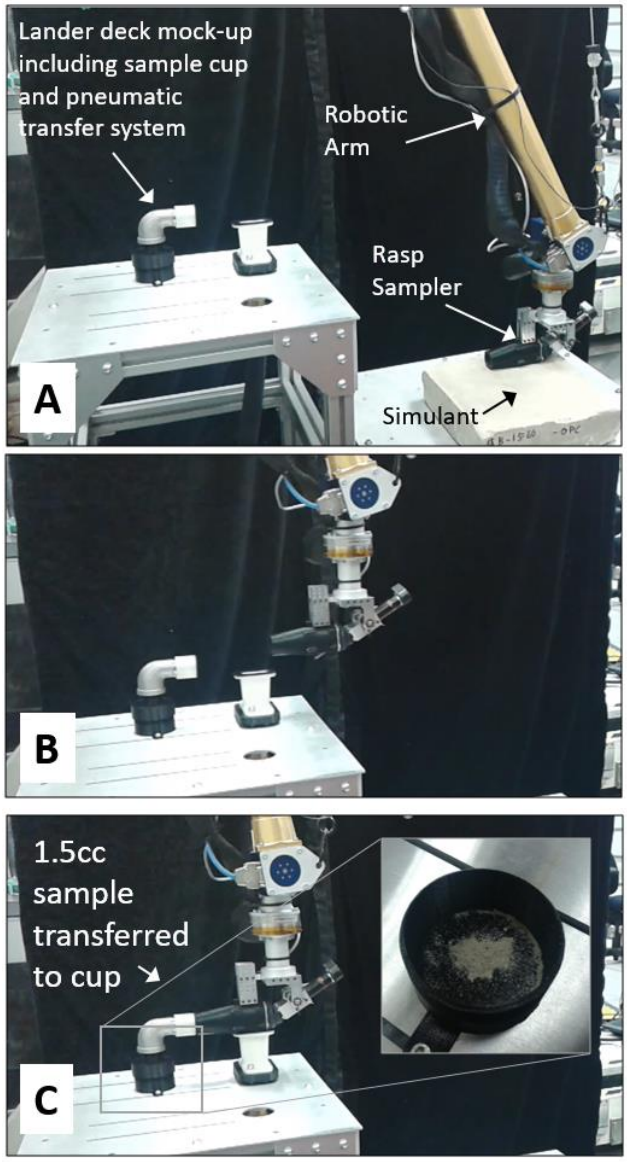

Figure 21. End-to-end sample excavation, acquisition, and transfer to a notional lander located instrument cup was successfully demonstrated for the Rasp Sampling System. Image (A) shows Rasp in sample acquisition position with bottom face of sampler against ground while cutter is operated. (B) Shows the Rasp in an intermediate position prior to pneumatic transfer system and instrument cup/inlet docking. (C) Shows the sample transfer step and a close-up of the material transferred to the instrument cup.

9. SAMPLE TRANSFER

The very low surface gravity of Enceladus represents additional challenges for sample handling and transfer from the place where it is collected to the place where it has to be eventually deposited. Past missions to different planetary bodies made use of the local gravity to handle the sample. The Mars Science Laboratory rover moves the robotic arm with respect to the gravity vector and adopts a combination of percussion and vibration mechanisms to transfer the sample powder from the drill to the instruments [Jandura, 2012]. The Phoenix lander exploited the Mars gravity to deliver the sample collected to the instruments by just pouring it [Bonitz, 2008]. On Enceladus, it is not possible to rely on gravity to handle the sample. For this reason, other methods have to be considered. Which method is better depends on the type of sampling system adopted. As an example, a scoop would probably require a scraping system.

There are sampling systems which enclose the sample and these systems require a method to force the sample out of the container where it is collected. One of the emerging methods for sample handling in very low gravity environments is the use of pneumatics. Such a method is being adopted by the OSIRIS-REx spacecraft to collect loose samples from the surface of the asteroid Bennu [Boshore, 2015]. For this reason, an air-based pneumatic sample transport system has been designed and tested to evaluate its feasibility in the case of using enclosed sampling systems (e.g., rasp, front-face concave powder bit). The aim of using this method is to force the sample out of the place where it is collected and to follow a predefined path to reach its final destination. The same general working principle was considered for both the rasp and the front-face concave powder bit. The system is composed of three main components: the air tank, the sampling tool and the sample chamber (Fig. 22). The air tank, the sample chamber and their respective fittings are fixed in place, while the sampling tool can be coupled to the system via sealed connection points to close the pneumatic circuit. Both sampling tools were co-designed for both sampling and pneumatic transfer purposes (Fig. 23 and Fig. 24).

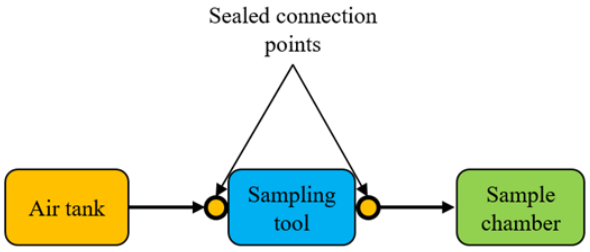

Figure 22. Pneumatic sample transfer system schematic

The sample chamber was provided with venting holes and a filter to let the gas escape but retain the sample inside. A first approximation analytical model of the pneumatic system was developed to study the physics of the sample transport and to provide guidelines that helped in designing the system. The input parameters for the analytical model were an average particles density of 2500 kg/m3, an average particles diameter of 500 μm and a particles mass flow rate of 10 g/s. An inlet pressure of about 4.1 bar (60 PSI) for the rasp and 6.9 bar (100 PSI) for the front-face concave powder bit were obtained as a trade-off between the pressure losses and the velocity required to achieve a dilute phase transport of the powders. Since the internal volume of the rasp is significantly bigger than the one of the front-face concave powder bit, the air volume flow rate obtained was 425 l/min (15 CFM) for the former and 5.6 l/min (0.2 CFM) for the latter. The end-to-end sampling chain, from sample collection to sample transfer, was experimentally tested showing satisfactory preliminary results: the pneumatic system was able to transfer samples ranging from coarse-grained (on the order of magnitude of 500 μm) to fine-grained (on the order of magnitude of 100 μm) simulant aggregates achieving the transferring of the minimum sample volume required.

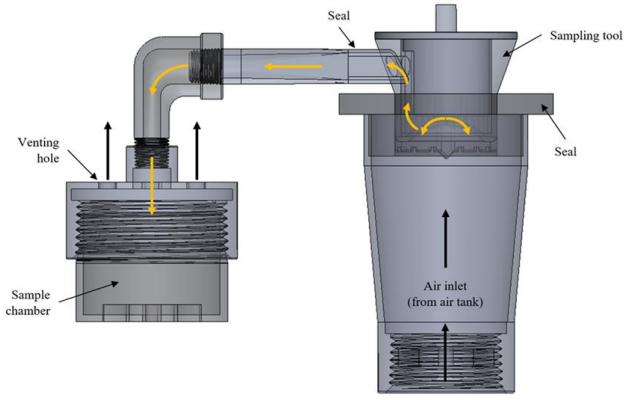

Figure 23. Pneumatic sample transfer system design implemented for the front-face concave powder bit. The bold black arrows represent the flow of clean air, the bold orange arrows represent the flow of the air and powder/sample mixture.

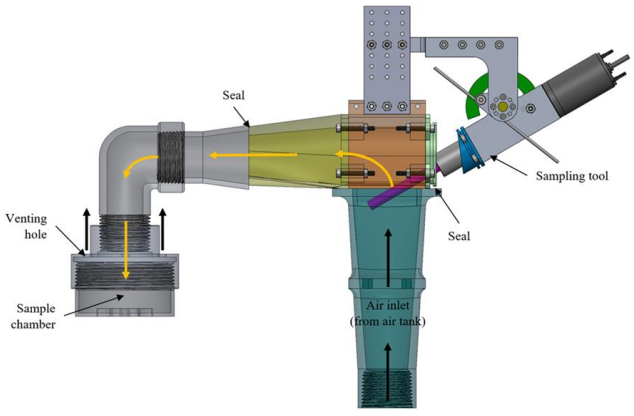

Figure 24. Pneumatic sample transfer system design implemented for the rasp sampling tool. The bold black arrows represent the flow of pure air, the bold orange arrows represent the flow of the air and powder mixture.

10. Conclusions and Future work

A series of sampling devices for sample acquisition and sample transfer and handling mechanisms applicable to an Enceladus surface environment was presented. Low fidelity prototypes were developed and tested and it was demonstrated that they can be operated with very low preload forces, in the 6 to 10N range, and able to collect the desired volume of sample material.

The devices are being further developed with expectation for the results and operational requirements to be compared, and then an end-to-end sampling system of higher fidelity would be developed for evaluation.

Acknowledgements

Research reported in this paper was conducted at the Jet Propulsion Laboratory (JPL), California Institute of Technology under a contract with National Aeronautics Space Administration (NASA).

References

[1] L. Jandura et al., Collecting Samples in Gale Crater, Mars; an Overview of the Mars Science Laboratory Sample Acquisition, Sample Processing and Handling System, Space Science Reviews 170 (1-4), 2012.

[2] R. G. Bonitz et al., NASA Mars 2007 Phoenix Lander Robotic Arm and Icy Soil Acquisition Device, Journal of Geophysical Research: Planets 113 (E3), 2008.

[3] E. Beshore et al., The OSIRIS-REx asteroid sample return mission, IEEE Aerospace Conference, Big Sky (Montana, USA), 2015.

[4] Molaro J. L., Meirion-Griffith G., Phillips C. B., Mitchell K. L., Hodyss R., et al., " Microstructural Evolution of Solar System Ices Through Sintering," #2977, 49th Lunar and Planetary Science Conference, 2018.

[5] K. Edelberg , P. Backes, J. Biesiadecki, S. Brooks, D. Helmick, W. Kim, T. Litwin, B. Metz, J. Reid, A. Sirota, W. Ubellacker and P. Vieira, "Software System for the Mars 2020 Mission Sampling and Caching Testbeds", IEEE Aerospace Conference, 2018.

[6] S. W. Squyres, K. Nakamura-Messenger, D. F. Mitchell, V. E. Moran, M. B. Houghton, D. P. Glavin, A. G. Hayes, D. S. Lauretta, and the CAESAR Project Team, "THE CAESAR NEW FRONTIERS MISSION: 1. OVERVIEW," 49th Lunar and Planetary Science Conference(LPI Contrib. No. 2083), 2018.

[7] R. Bonitz, "The Brush Wheel Sampler - a Sampling Device for Small-body Touch-and-Go Missions," Proc. IEEE Aerospace Conference, 2012.

[8] P. Backes, C. McQuin, M. Badescu, A. Ganino, H. Manohara, Y. Bae, R. Toda, N. Wiltsie, S. Moreland, J. Grimes-York, P. Walkemeyer, E. Kulczycki, C. Dandino, R. Smith, M. Williamson, D. Wai, R. Bonitz, A. San Martin, and B. Wilcox, "Sampling System Concepts for a Touch-and-Go Architecture Comet Surface Sample Return Mission," AIAA SPACE 2014 Conference and Exposition, 2014.

[9] Ercoli Finzi, A. Bernelli-Zazzera, Franco Dainese, C. Malnati, F. Magnani, Paola Re, E. Bologna, P. Espinasse, S. Olivieri, A. (2007). SD2 - How to sample a comet. Space Science Reviews. 128. 281-299. 10.1007/s11214-006-9134-6.

[10] Seweryn, K., Grygorczuk, J., Rickmann, H., Morawski, M., Aleksashkin, S., Banaszkiewicz, M., Drogosz, M., Gurgurewicz, J., Kozlov, O., Krolikowska, M., Sutugin, E. S., Wawrzaszek, R., "CHOMIK Sampling Device of Penetrating Type for Russian Phobos Sample Return Mission," 2010.

BIOGRAPHY

Mircea Badescu *is a Technologist at the Jet Propulsion Laboratory. He received the Ph.D. degree in robotics in mechanical and aerospace engineering, from Rutgers University, in 2003. He has experience on planetary and low gravity sampling systems, extreme environments devices, power ultrasonic piezoelectric devices integration, instruments for planetary exploration, optical components for telescopes, optimal design of self-reconfigurable robots using parallel platforms as modules, haptic devices and scuba diving equipment. He has experience in organizing and conducting field tests including glaciers, Antarctica, and desert. He is coauthor of 106 publications, 17 patents, 71 NTRs, and received 47 NASA and Tech Brief awards.*

Scott Moreland, Ph.D. *received the B.S. degree from University of Toronto and M.S. and Ph.D. degrees in Mechanical Engineering from Carnegie Mellon University and joined JPL in 2013. His expertise is primarily in robotic systems that interact with the ground for mobility or sampling. His experience includes the design and fielding of robotic vehicles, mechanism design, and mechanical systems testing.*

Paul Backes *is the Group Supervisor of the Robotic Manipulation and Sampling group at Jet Propulsion Laboratory, California Institute of Technology, where he has been since 1987. He received the BSME degree from U.C. Berkeley in 1982, MSME degree from Purdue University in 1984, and Ph.D. in Mechanical Engineering from Purdue University in 1987. Dr. Backes received the 1993 NASA Exceptional Engineering Achievement Medal for his contributions to space telerobotics, 1998 JPL Award for Excellence, 1998 NASA Software of the Year Award Sole Runner-up, 2004 NASA Software of the Year Award, and 2008 IEEE Robotics and Automation Award. He has served as an Associate Editor of the IEEE Robotics and Automation Society Magazine.*

Alexander Brinkman *received his M.S in Robotic Systems Development from Carnegie Mellon's Robotic Institute. He joined the Robotic Manipulation and Sampling group at Jet Propulsion Laboratory in 2017 where he develops manipulation software and autonomous capabilities to enable future sampling missions to Europa, Enceladus, Mars, and comets.*

Jamie Molaro *is a planetary scientist at the Planetary Science Institute and the Caltech/Jet Propulsion Laboratory. She received her PhD in Planetary Science from the University of Arizona in 2015. Her research focuses on physical weathering processes and landscape evolution on rocky and icy solar system objects. She employs thermal and mechanical numerical modeling as well as laboratory investigations in her work, and is an expert on the properties of ice/rocks and regolith on airless body surfaces.*

Dario Riccobono *received both the B.S. and the M.S. degree in Aerospace and Astronautic Engineering from the Politecnico di Torino (Italy), where he is currently pursuing a Ph.D. in Mechanical Engineering. His primarily expertise is in robotic systems for mobility and sampling. His experience includes mechanical systems analysis, design and testing, as well as space mission analysis and design.*

Dr. Mathieu Choukroun *is a planetary scientist whose primary research aims at better understanding the exchange processes that take place between the interior and the surface (or atmosphere/coma) of icy worlds and comets. This research involves experimental investigation of the physical and chemical properties of icy materials, and thermodynamic and geophysical modeling of icy worlds and cometary environments to apply the experimental results.*

Giancarlo Genta *received the degree in Aeronautical and Aerospace Engineering from the Politecnico di Torino (Italy). He has been full professor of Machine Design and Construction at the Politecnico di Torino for over 30 years. His areas of professional interest include vibration, vehicle design, magnetic bearings, rotordynamics, and space electric propulsion. His awards include the Yangel Medal (2013) and the Engineering Science Award of the International Academy of Astronautics (2013). He is author of over 350 papers, 4 patents, and 21 books in the fields of education, science divulgation, and science fiction.*